



Since January 2020 Elsevier has created a COVID-19 resource centre with free information in English and Mandarin on the novel coronavirus COVID-19. The COVID-19 resource centre is hosted on Elsevier Connect, the company's public news and information website.

Elsevier hereby grants permission to make all its COVID-19-related research that is available on the COVID-19 resource centre - including this research content - immediately available in PubMed Central and other publicly funded repositories, such as the WHO COVID database with rights for unrestricted research re-use and analyses in any form or by any means with acknowledgement of the original source. These permissions are granted for free by Elsevier for as long as the COVID-19 resource centre remains active.



## The influence of collagen film nanostructure on pulmonary stem cells and collagen–stromal cell interactions

Chun-Jen Huang<sup>a,1</sup>, Yi-Lun Chien<sup>a,b</sup>, Tai-Yen Ling<sup>a,2</sup>, Huan-Chien Cho<sup>a,c</sup>, John Yu<sup>a,d,\*</sup>, Ying-Chih Chang<sup>a,\*</sup>

<sup>a</sup> Genomics Research Center, Academia Sinica, Taipei 115, Taiwan

<sup>b</sup> Institute of Bioscience and Biotechnology, College of Life Sciences, National Taiwan Ocean University, Keelung 202, Taiwan

<sup>c</sup> Institute of microbiology and immunology, National Yang-Ming University, Taipei 112, Taiwan

<sup>d</sup> Institute of Cellular and Organismic Biology, Academia Sinica, Taipei 115, Taiwan

### ARTICLE INFO

#### Article history:

Received 10 May 2010

Accepted 7 July 2010

Available online 1 August 2010

#### Keywords:

Pulmonary stem/progenitor cells

Nanostructures

Extracellular matrix

Collagen I structure

Atomic force microscopy

Cell culture

### ABSTRACT

We have recently identified a rare subpopulation of lung colony cells with the characteristics of pulmonary stem cells, and discovered that stem cell colonies grew preferentially on type I collagen films in a serum-free medium. In order to further optimize culture conditions and determine stem cell growth in relation to microenvironments (including the stroma, medium and nanostructures of type I collagen films), both primary and pre-sorted stem cells were cultured on the type I collagen films with controllable degree of polymerization and film thickness, as confirmed by an atomic force microscope and surface profiler. We found that in a primary culture, the spreading of stromal cells is greatly restrained and both the size and number of colonies are significantly reduced on highly polymerized collagen films. In contrast, in a pre-sorted stem cell culture without stromal cells, the intrinsic stem cell properties and cell number are independent of the degree of collagen polymerization. Our results indicate that the nanostructures of type I collagen films primarily affect stem colony formation through the collagen–stroma interactions. In those cases, collagen film thickness shows no effect on colony formation.

© 2010 Elsevier Ltd. All rights reserved.

### 1. Introduction

Stem cells are of great potential in molecular biology research and regenerative medicine [1]. Their defining characteristics include the potential for proliferation and differentiation into various cell types. Recently, Ling et al. discovered a rare subpopulation of pulmonary cells at bronchoalveolar junctions of lung tissues, exhibiting slow cycling and Octamer-4 (Oct-4<sup>+</sup>) expressing [2]. Oct-4, a member of the family of POU-domain transcription factors, is an important regulator of self-renewal in pluripotent embryonic stem cells. The cells have been revealed as lung stem cells that form epithelial colonies in a serum-free culture and are able to differentiate into type I and II pneumocytes. In addition, they are prone to infection of the severe acute respiratory syndrome-associated coronavirus (SARS-CoV) [2,3]. These findings are promising in drug screening, tissue engineering and functional genomics. Therefore, a robust and consistent cell culture system should be

established to provide moderate to large numbers of cells on a routine basis [4–7]. Ling et al.'s earlier screening has determined that thin films of type I collagen on the tissue culture polystyrene (TCPS) plates is most effective in forming high density colony cells [2]. However, the interactions of lung stem cells with their micro-environment remain obscure and need to be elucidated.

Type I collagen is a long, fibrous structural protein, found in all multi-cellular animals as a major protein in extracellular matrix (ECM). A collagen monomer consists of three left-handed helices which arrange to an extended superhelix with roughly 1.5 nm in diameter and 300 nm in length. The monomers can spontaneously self-assemble in vivo and in vitro into fibrils with a periodicity of 67 nm, ranging 10–500 nm wide and up to several microns long. The spatial distribution and aggregation states of collagens have found to mediate the cellular signaling and development, through integrins recognitions [8,9]. For example, the fibrillar structures of type I collagen have led to distinctive changes in gene expression, population, and morphological profiles of cultured smooth muscle cells (SMCs) [10–13]. The heat-denatured type I collagen (denatured collagen), whose ordered three-dimensional structure is destroyed [14], promotes SMC cellular proliferation and spreading [15], while native type I collagen (native collagen) inhibits its growth [10,15]. Further mechanistic study suggested that native collagen suppresses cyclin E-associated kinase and cyclin-dependent kinase 2 (Cdk2)

\* Corresponding authors. Genomics Research Center, Academia Sinica, Taipei 115, Taiwan. Tel.: +886 2 27871277; fax: +886 85020632.

E-mail address: [yingchih@gate.sinica.edu.tw](mailto:yingchih@gate.sinica.edu.tw) (Y.C. Chang).

<sup>1</sup> Present address: Austrian Institute of Technology, Donau-City-Strasse 1, 1220 Vienna, Austria.

<sup>2</sup> Present address: Institute of Pharmacology, College of Medicine, National Taiwan University, Taipei 100, Taiwan.

phosphorylation while increasing levels of the Cdk2 inhibitors p27<sup>Kip1</sup> and p21<sup>Cip1/waf1</sup>. As a result, proliferation of SMCs is arrested in the G1 phase of the cycle [10].

The stromal cells surrounding the pulmonary stem cell colonies were found to have similar characteristics with mesenchymal cells carrying the  $\alpha$ -smooth muscle actin marker [2]. It is therefore advantageous to engineer collagen substrates with distinct nanostructures in order to understand the effects to the stromal cells and, consequently, the pulmonary stem cell formation in the stem cell–stromal cell co-culture. By adopting the previously developed methods with minor adjustment [12], both native and heat-acid denatured collagen thin films were readily prepared under various collagen solution concentrations. We have characterized the surface thin film morphology, the fibrillar formation, and the film thickness with atomic force microscopy (AFM), and surface profiler. Moreover, the cultivation of pre-sorted colony cells allowed us to observe the exclusive interaction between colony cells and type I collagen films. The correlation among stem cells, stromal cells and biomaterials is revealed by monitoring the number and size of colonies and performing immunohistochemical staining for Oct-4 and  $\alpha$ -smooth muscle actin.

## 2. Materials and methods

### 2.1. Pulmonary primary cell culture

To begin with, neonatal imprinting control region (ICR) mice's lungs were removed, diced and washed with Hank's buffer solution containing penicillin (10 units/ml) and streptomycin (100  $\mu$ g/ml) (both from Sigma–Aldrich, St. Louis, MO). The lung pieces were soaked overnight in Joklik's minimum essential medium (JMEM; Sigma–Aldrich) with 0.1% protease type-XIV (Sigma–Aldrich) at 4 °C. Subsequently, they were transferred to 10% fetal calf serum (FCS)/JMEM, pipetted several times to release pulmonary cells and then filtered through a 100- $\mu$ m nylon cell strainer. The released cells, with approximately  $1.0\text{--}1.5 \times 10^6$  nucleated cells per neonatal mouse, were washed and re-suspended in an MCDB-201 medium containing insulin-transferrin-selenium (ITS) supplements (Bibco, Grand Island, NY). These cells were diluted to a density of  $3 \times 10^5$  cells/ml, and seeded 1 ml per well for a 24-well plate. After 1 day of incubation, the primary cultures were washed with MCDB-201 medium to remove unattached cells. Finally, both fresh medium with ITS supplement as well as epidermal growth factors (EGF), (1 ng/ml, Invitrogen, Carlsbad, CA) were added. The cells were incubated in 5% CO<sub>2</sub> at 37 °C for eight days, and then the colony was examined for quantification.

### 2.2. Preparation of collagen films

Original rat-tail type I collagen (BD Biosciences, San Jose, CA) was stocked in 0.02 N acetic acid (Sigma–Aldrich) in order to prevent polymerization. To prepare the native collagen, original rat-tail type I collagen (0.8 ml, ~4 mg/ml) was neutralized with  $10\times$  Ca<sup>2+</sup>- and Mg<sup>2+</sup>-free Dulbecco's phosphate buffered saline (DPBS; Invitrogen) (0.1 ml) and NaOH (0.1 N, 0.1 ml). To prepare the denatured collagen, original rat-tail type I collagen (~4 mg/ml) was mixed with 0.4 M acetic acid,  $10\times$  DPBS in a 16:1:2 ratio. The mixture was boiled for 30 min and neutralized with 1 N NaOH. The collagen concentration was then adjusted to 3.88 mg/ml with  $10\times$  DPBS. All concentrations of native and denatured collagen were prepared by serial 2.5-fold dilution with  $1\times$  DPBS. Throughout the preparation process, all solutions were stored in ice to minimize polymerization until collagen was applied to 24-well TCPS plates (Corning Incorporated, Acton, MA). The surface area of the well bottom was 1.9 cm<sup>2</sup>. 180- $\mu$ l collagen solutions with initial concentrations of 0, 0.016, 0.04, 0.1, 0.25, 0.62, 1.55 and 3.88 mg/ml were dispensed and covered the well surfaces. They were then air-dried overnight in a sterile hood to deposit collagen onto TCPS surfaces, rinsed thrice with  $1\times$  DPBS to remove non-adherent collagen and stored in  $1\times$  DPBS at 4 °C. Before use, they were rinsed once again with deionized (DI) water and air-dried in a hood. For the convenience, the collagen samples in this study are denoted by their native or denatured state and their initial solution concentrations, such as "denatured, 3.88 mg/ml".

### 2.3. AFM

AFM images of collagen thin films were recorded in air using the MFP-3D-BIO AFM (Asylum Research, Santa Barbara, CA). The AFM was operated in AC mode using the POINTPROBE-PLUS Silicon cantilevers (force constant of 42 N/m and resonant frequency of 330 kHz, Nanosensors, Neuchatel, Switzerland). Before scanning, the collagen samples were rinsed with DI water to remove salts, and dried overnight in a laminar flow sterile hood.

### 2.4. Surface profiler

A KLA Tencor P-16+ surface profiler (San Jose, CA) was used to measure surface thickness. The stylus tip size was 2  $\mu$ m in diameter. Applied force, scan speed, sampling rate and scan length were 1 mg, 20  $\mu$ m/s, 200 Hz and 1000  $\mu$ m, respectively. To prepare the surface for measurement, a thin stripe was taped to the polystyrene plate in advance to prevent partial surface contact with the collagen solution. After the collagen solution in the plate was air-dried in the sterile hood, the tape was removed to expose a bare TCPS surface. The differences in thickness between the bare TCPS and collagen films were measured.

### 2.5. Quantification of colony cells

Surface tension contributes to a thick and heterogeneous collagen layer in the peripheral area on each well of the 24-well plate; only the central collagen layer within a 5 mm-radius is uniform and flat. Therefore, to obtain credible results, the quantitative cell counts, AFM and surface profiler scans were performed on the central area. The numbers of colonies with the comprising cell number ranges of below 25, between ~25 and ~100, and between ~100 and ~250 were counted separately.

### 2.6. Immunocytochemistry

Immunocytochemical staining was performed to examine the cell characteristics [2] on collagen films. Cells in primary cultures were washed three times with phosphate buffered saline (PBS), and then placed in methanol:acetone at 1:1 for 2 min on ice. The cells were incubated with primary mouse antibody against the antigens of  $\alpha$ -smooth muscle actin (DakoCytomation, Glostrup, Denmark) and primary rabbit antibody against Oct-4 (Santa Cruz, CA) at 4 °C. After an overnight incubation, the cells were washed with PBS, and then incubated for 1 h at room temperature with secondary antibodies of goat anti-rabbit IgG conjugated with Cy3 (Jackson ImmunoResearch, West Grove, PA) and goat anti-mouse IgM conjugated with FITC (Jackson ImmunoResearch), respectively. Finally, the cells were counter-stained with 4',6-diamidino-2-phenylindole (DAPI) for 10 min at room temperature.

### 2.7. Colony cell isolation

The colony cell isolation protocol was developed as previously reported [2] with the following modification. A quantity of  $1 \times 10^7$  cells was collected from the primary culture after an 8-day incubation and washed in PBS, 3% FBS. Since the pulmonary stem cell positively expresses specific markers of CXC chemokine receptor (CXCR4) and intercellular adhesion molecule-1 (CD54) on the cell membrane, both stains were applied according to standard procedures. The cells were incubated in a polyclonal goat CXCR4 antibody (10  $\mu$ g/ml, Abcam, Cambridge, UK) for 30 min at 4 °C and then washed with PBS, 3% fetal bovine serum (FBS). Thereafter, the cells were incubated with a Cy5-conjugated donkey anti-goat secondary antibody (7.5  $\mu$ g/ml, Chemicon, Temecula, CA) for 30 min at 4 °C and then washed with PBS, 3% FBS. For the second staining, the cells were incubated with a monoclonal R-Phycoerythrin (R-PE)-conjugated hamster anti-mouse (ICAM-1) CD54 antibody (4  $\mu$ g/ml, BD Biosciences) for 30 min at 4 °C and then washed with PBS, 3% FBS. They were then stained with propidium iodide (PI) (1  $\mu$ g/ml, Sigma–Aldrich) to allow exclusion of nonviable cells. The pulmonary stem cells were sorted on a FACS-Vantage-SE flow cytometry system (BD). The sorted stem cells were re-seeded in DMEM medium containing 10% FBS (Sigma–Aldrich) and 1% ITS, and MCDB-201 medium containing 1% ITS and 1 ng/ml EGF, respectively. The density was  $5 \times 10^4$  cells/well for 12-well plates, which were pre-coated and air-dried with native and denatured collagen, (both at a concentration of 3.88 mg/ml), for each culture medium.

## 3. Results

### 3.1. Thickness and nanostructures of collagen films

The thickness of both native and denatured collagen films was measured by a surface profiler. The average thickness of collagen films on TCPS increased exponentially with the initial concentrations (Fig. 1A). Native collagen films, however, were roughly twice as thick as denatured films with identical initial concentrations. For example, the thicknesses of samples of collagen (native, 3.88 mg/ml) and collagen (denatured, 3.88 mg/ml) were 226 nm and 100 nm, respectively. Collagen (native, 1.55 mg/ml) and (denatured, 1.55 mg/ml) were 24 nm and 14 nm, respectively. This difference can be attributed by the changes in physical properties of collagen solutions, as the polymerized native collagen solution conceivably is more viscous and less soluble, leading to porous structures in the films, than the denatured one thus precipitating thicker films. Due to

the surface roughness of TCPS (in the order of 1–10 nm), as the initial concentrations are below 0.1 mg/ml in native and 0.25 mg/ml in denatured collagen solutions, the resulting film thicknesses cannot be measured accurately. In these diluted samples, existence of collagen molecules at surfaces was imaged by AFM.

The AFM was utilized to examine the structures of collagen thin films at nanoscale resolution. For the samples prepared by native collagen solutions, surface morphology was significantly correlated to its initial concentration. In the film with low native collagen concentration, i.e. 0.62 mg/ml, fibrillar collagen did not distribute uniformly on the TCPS, and supramolecular collagen was not observed (Fig. 1B (i)). As the initial concentration was increased to 1.55 mg/ml, fibrillar collagen of ~200 nm in diameter appeared, and supramolecular collagen (approximately 1–2  $\mu\text{m}$  in diameter, black arrow in Fig. 1B (ii)) was observed to be formed by the twists of fibrils. With initial collagen solution at 3.88 mg/ml, the film was covered with supramolecules of adsorbed collagen (Fig. 1B (iii)). The thicker fibrillar structure is also confirmed by the Z-scale of 300 nm, compared with that of 100 nm for the other collagen films (0.62 mg/ml in Fig. 1B (i) and 1.55 mg/ml in Fig. 1B (ii)). These results suggest that both density and dimensions of the adsorbed collagen fibers are highly proportional to the initial concentrations of the native collagen solution.

To examine the detailed structures of native collagen, images of films at lower collagen concentrations (from 0.1 mg/ml to 0.62 mg/ml) in a  $5\ \mu\text{m} \times 5\ \mu\text{m}$  scan area were taken. As shown in Fig. 1B (iv–vi), these surfaces were covered with thin filaments (~50 nm in diameter, shown, blue arrows) that evenly dispersed. In addition, the density of these filaments depended on the initial concentration of the native collagen solution as well. Moreover, filaments seemed to provide anchors for fibrils whose diameter was gradually narrowing to the diameter of filaments in the end site as indicated by green arrows, similar to the previous findings [12,13].

In contrast, the nanostructures of the denatured collagen films showed less dependence on initial concentration and film thickness. With the scan area of  $50\ \mu\text{m} \times 50\ \mu\text{m}$ , the morphologies of denatured collagen films appeared relatively featureless (Fig. 1C (i)–(iii)). The features were almost identical to the image of the bare TCPS (Fig. 1C (iv)), indicating that the adsorbed collagen homogeneously covered the surface and only few accumulates appeared (red arrows in Fig. 1C (iii)). Within the scan area of  $5\ \mu\text{m} \times 5\ \mu\text{m}$ , no thin filaments were observed even at the highest denatured collagen concentration of 3.88 mg/ml (Fig. 1C (v)), except some small aggregates of denatured collagen molecules (~10 nm in diameter). These data suggest that once the collagen solution was denatured with heat and acid, collagen monomers were no longer able to self-assemble into collagen fibrils in collagen films regardless of its concentration.

### 3.2. Number and size of colony cells in serum-free primary cultures

To identify the colonies carrying the characteristics of stem cells on collagen surfaces with different treatments, we immunostained the cells cultured on native and denatured collagen samples. Our previous study has proved that the pulmonary epithelial stem cells express markers of Oct-4, stage-specific embryonic antigen-1 (SSEA-1), stem cell antigen-1 (Sca-1) and cytokeratin-7 [2]. The cells cultured on collagen films (native, 3.88 mg/ml) and (denatured, 3.88 mg/ml) were shown side by side (Fig. 2). Colony cells on the native collagen films expressed Oct-4 in the nuclei whereas the surrounding cells were negative (Fig. 2A–C). For cells on collagen (denatured, 3.88 mg/ml) (Fig. 2D–F), the same expression patterns were displayed. The identical results were found in other native and denatured samples with different initial concentrations. The findings showed the feasibility of the cultivation of pulmonary stem

colonies for the following examination on collagen films with additional pretreatment.

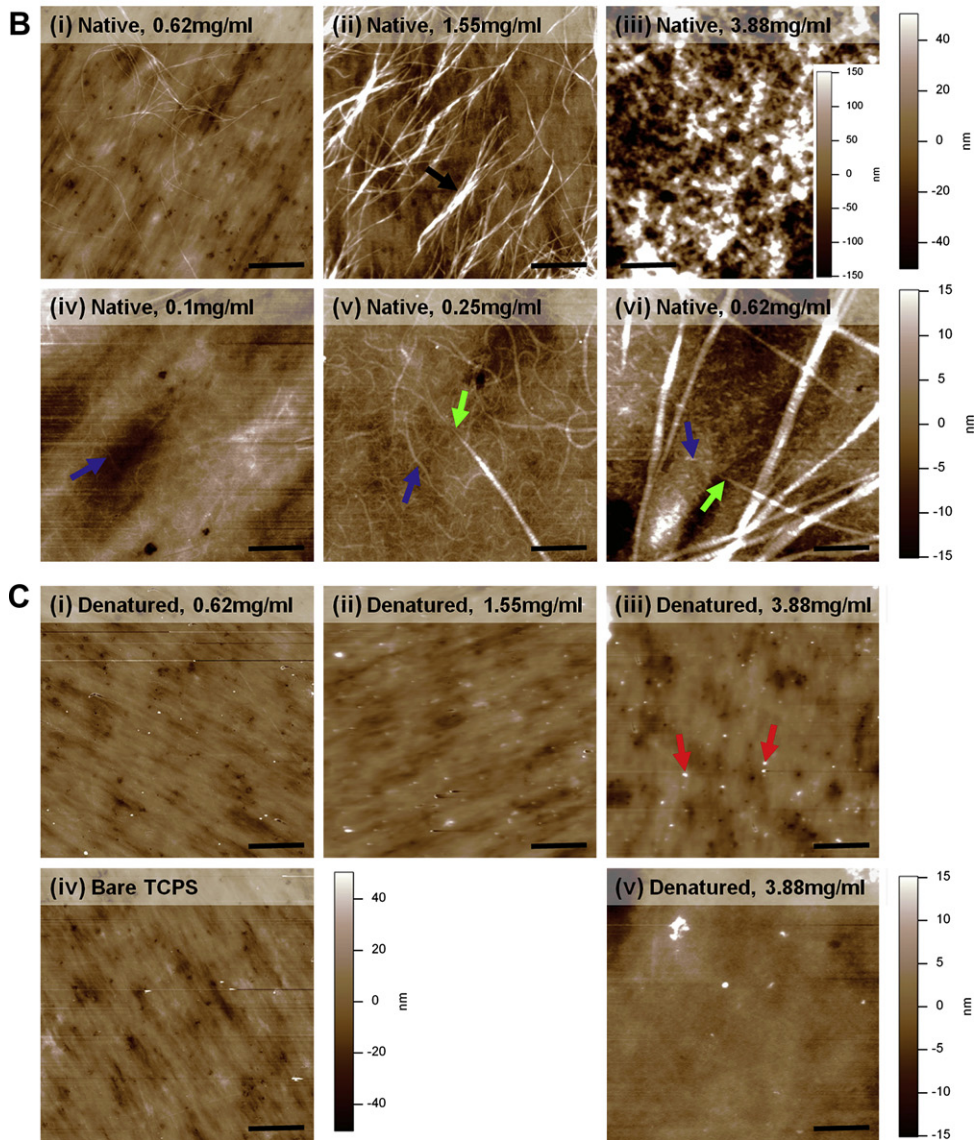
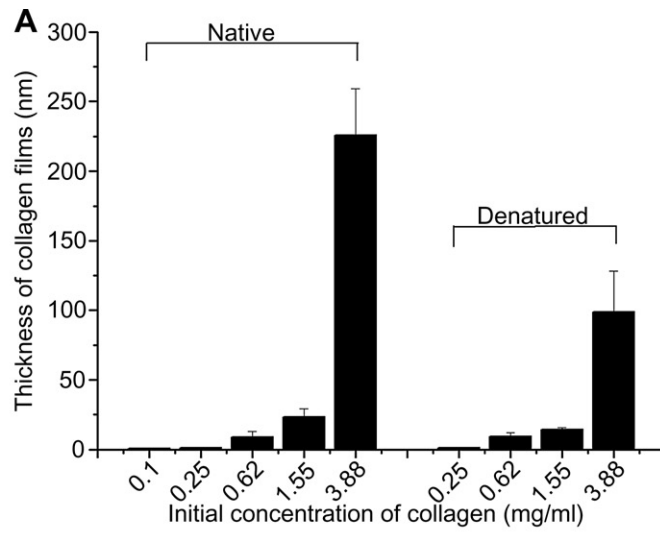
In order to study the effects of native and denatured collagen films on colony formation, the numbers and sizes of colonies on each sample were analyzed based on the following method as shown in Fig. 3. First, the number of colonies on each sample was counted over a fixed area of  $78.5\ \text{mm}^2$ . Secondly, the colonies on TCPS were grouped into three categories: fewer than 25 cells (bars in red), 25–100 cells (bars in green), and 100–250 cells per colony (bars in blue). Thirdly, to estimate the total stem cell counts in each sample, we derived an approximate value of individual total colony cell number from a weighted mathematical method. The median of each category,  $N_i$ , was estimated as the weighted value, e.g.  $N_i = 175$  for category of 100–250;  $N_i = 62.5$  for category of 25–100;  $N_i = 12.5$  for category of <25. The total cell number of each category,  $N_t$ , was obtained from multiplying  $N_i$  by the colony number,  $C_i$ , in that category as  $N_t = N_i \times C_i$ . The sums of the weighted  $N_t$  values of three categories for each sample are shown in Fig. 3A with the numbers indicated on the right-side y-axis. For the native collagen film samples, there was a rapid decrease in both colony numbers and sizes when the initial collagen solutions increased from 0.04 mg/ml to 3.88 mg/ml. However, for the denatured collagen samples, there was no dependence on the concentrations in stem cell colony counts (Fig. 3A). As comparing the colony size and number of colony cells cultured on TCPS without collagen coating, we observed the promotion of the stem cell growth resulting from the presence of collagen molecules. Phase contrast images of primary cell cultures on collagen films are presented in Fig. 3B. The flat and high spreading stromal cells surrounded the cluster of stem cells that slightly lose optical focus under microscope observation due to their round up shapes.

Overall, the quantities of stem cell colonies on all denatured collagen films were consistently abundant compared with those on the native collagen film samples, and the correlation with their thicknesses was not found. The sizes of the stem cell colonies formed on all denatured collagen film samples were larger than those on the native collagen films with higher initial collagen concentrations of 0.25–3.88 mg/ml. The surface difference as tracked by a surface profiler and AFM suggests that the nano-texture of collagen surfaces was the dominant factor regarding colony formation and existence in primary cultures. The presence of abundant collagen fibers apparently restricts the density and size of stem cell colonies.

### 3.3. Morphologies of stromal and colony cells in serum-free primary cultures

To understand how surface nanostructures can determine cell growth, the primary cultures were prepared on films of collagen (native, 3.88 mg/ml), (denatured, 3.88 mg/ml), and bare TCPS, respectively. First, the stromal cell morphologies on each sample were observed by immunostaining (in green), together with the optical phase contrast images. Cell spreading of the stained cells with  $\alpha$ -smooth muscle actin was markedly decreased and formed a constrictive shape on the native collagen film (Fig. 4A), compared with cells on the denatured collagen surface (Fig. 4B). It appears that the spreading of stromal cell was constrained on the collagen supramolecule structured film.

We also observed stromal cells spreading on a TCPS (two cells leaned against each other in Fig. 4C). Without collagen coating, the cell area of stroma was smaller than that on the denatured collagen films, which may be due to the absence of adhesion-promoting molecules on TCPS [16–18]. Moreover, we examined stem cell morphologies under identical culture conditions. The shape and size of the individual colony cell appeared similar on native and denatured collagen and TCPS surfaces. All colony cells appeared to be spherical shapes that are not fully spread on surfaces, which is



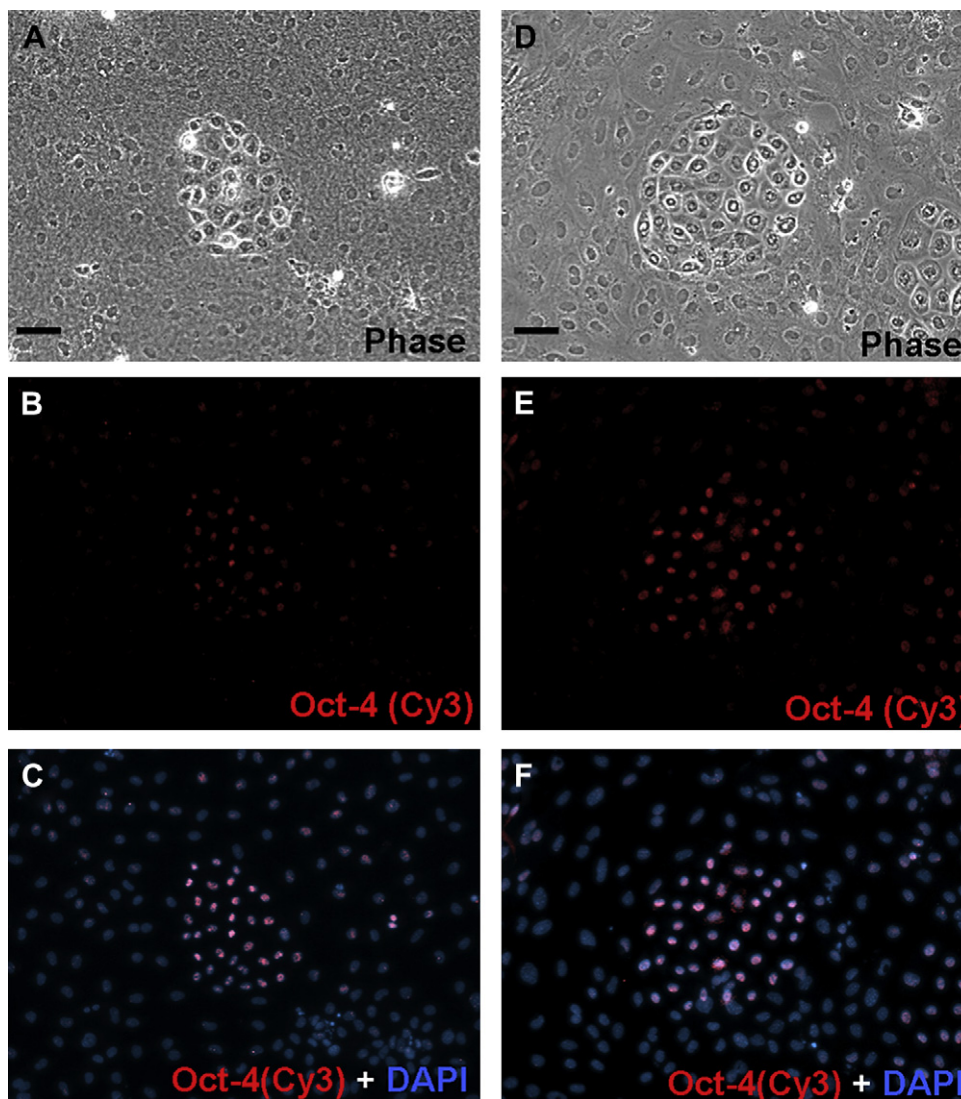


**Fig. 2.** Images of primary pulmonary cultures on native (A–C) and denatured (D–F) collagen films with an initial concentration of 3.88 mg/ml. A and D: bright field, B and E: immunostaining with Oct-4 (red), C and F: counterstained with DAPI (blue) The bars shown in A and D are 50  $\mu\text{m}$ .

similar to the morphology found in other stem cells [19,20]. Conceivably, the lack of adhesiveness of the colony cells might be the reason that their morphologies are not influenced by the collagen nanostructures as much as those of stromal cells.

#### 3.4. Sorted stem cells on collagen films with and without serum medium

In order to further understand the interactions among supporting substrates, stromal cells and pulmonary stem cells upon

different collagen nanostructures, the pulmonary colony cells were isolated from the primary cell culture. The sorting experiment was accomplished by collecting the cells with specific surface markers, CXCR4 and CD54, on a flow cytometry followed by re-seeding on the films (native, 3.88 mg/ml and denatured, 3.88 mg/ml). In addition, the sorted colony cells were incubated in DMEM with 10% FBS (Fig. 5A and C) and in serum-free MCBD-201 medium (Fig. 5B and D). After incubation for 7 days, the sorted cells were immunostained with Oct-4 to examine the preservation of the stem cell function. In the serum-containing DMEM, sorted cells expressed

**Fig. 1.** The thickness and nanostructures of collagen films. A: The thickness of collagen films measured by a surface profiler. Samples were prepared and patterned as described in the Materials and Methods section. Thickness is defined as the height difference between the bare TCPS and air-dried collagen films. All error bars show the standard deviation for four-time measurements. B: (i–iii) AFM images of collagen films in the scan area of  $50\ \mu\text{m} \times 50\ \mu\text{m}$  and prepared from native collagen solution at 0.62, 1.55, and 3.88 mg/ml (i, ii, and iii, respectively). The black arrow indicates formation of supramolecular collagen from fibrillar collagen. The bars shown in (i–iii) are 10  $\mu\text{m}$ . (iv–vi): AFM images of collagen films in the scan area of  $5\ \mu\text{m} \times 5\ \mu\text{m}$  prepared from native collagen solution with initial concentrations at 0.1, 0.25, and 0.62 mg/ml (iv, v, and vi, respectively). The blue arrow indicates thin filaments observed under fibrils. The green arrow shows fibrils, whose diameter is gradually narrowing to the diameter of filaments in the end site. The bars shown in (iv–vi) are 1  $\mu\text{m}$ . C: (i–iii): AFM images of collagen films in the scan area of  $50\ \mu\text{m} \times 50\ \mu\text{m}$  prepared from denatured collagen solution with the initial concentrations of 0.62, 1.55, and 3.88 mg/ml (i, ii, and iii, respectively). The red arrow shows round-shaped aggregates of denatured collagen. The bars shown in (i–iii) are 10  $\mu\text{m}$ . (iv): AFM image of bare TCPS surface in the scan area of  $50\ \mu\text{m} \times 50\ \mu\text{m}$ . The bar is 10  $\mu\text{m}$ . (v): AFM image of collagen film in the scan area of  $5\ \mu\text{m} \times 5\ \mu\text{m}$  prepared from denatured collagen solution with an initial concentration at 3.88 mg/ml. The bar is 1  $\mu\text{m}$ . The Z scales of the AFM images: For B (i, ii) and C (i–iv), the Z scales are 100 nm; for B (iii), the Z scale is 300 nm; for B (iv–vi) and C (v), the Z scales are 30 nm.

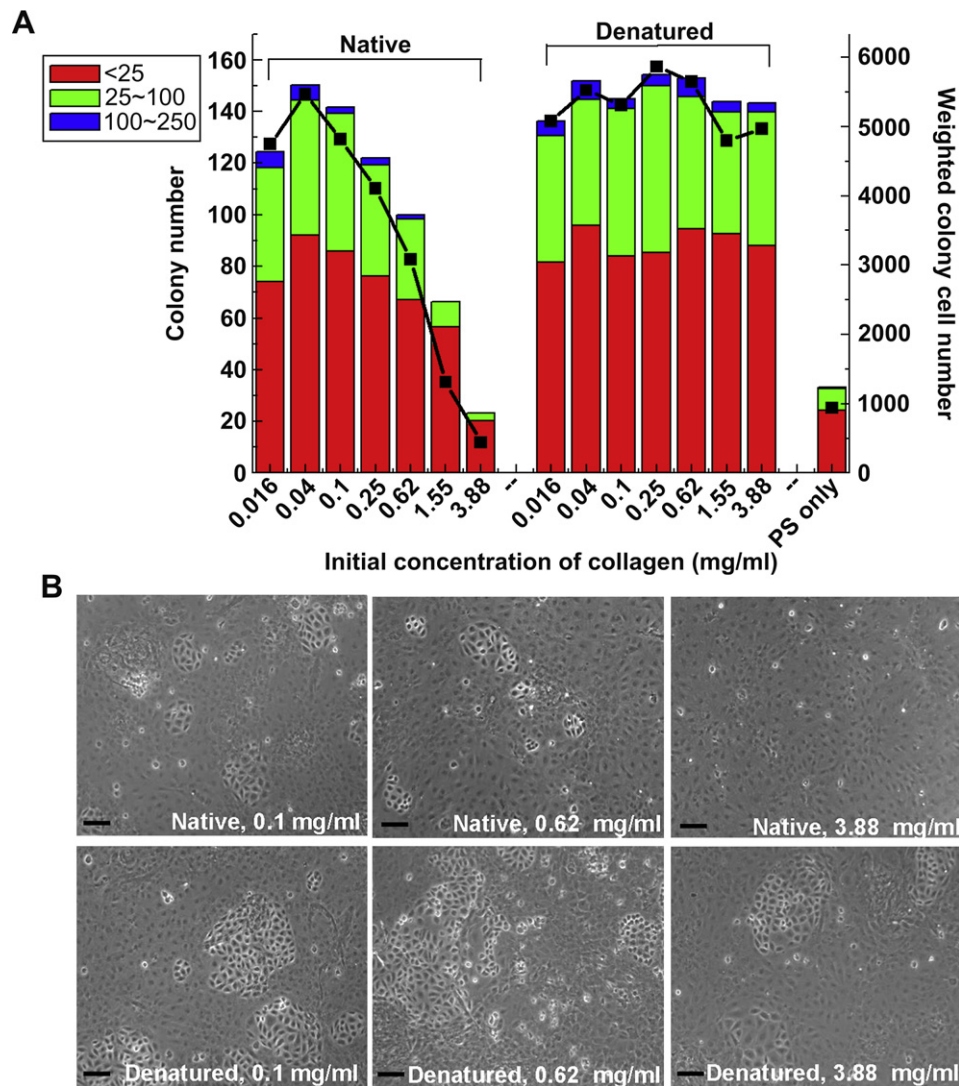


**Fig. 3.** Surface effects on the formation of pulmonary stem cell colonies. A: The colony counts and size distribution, as grouped by the cell number within each colony: (<25 cells/colony; 25–100 cells/colony; 100–250 cells/colony). The bars represent the colony number, and black solid squares show the weighted colony cell number. B: Optical phase images of pulmonary epithelial primary cells cultured on the films of native or denatured collagen with different initial concentrations. All images were taken on day eight. All bars are 100  $\mu$ m.

the Oct-4 marker and cell population became independent of the underlying collagen nanostructures (Fig. 5A and C). In contrast, in the original serum-free MCDB-201, the self-renewal ability of sorted cells was restrained and cells underwent differentiation (Fig. 5B and D). Our observation showed that in the case of sorted colony cells, cell fate is determined by medium components as opposed to collagen nanostructures.

#### 4. Discussion

Stem cells are highly controlled by specific microenvironments known as “niches” in vivo and, hence, substantial advances in cell culture methodology and understanding of ECM in vitro are essential to lead to enormous potential of stem cells. This study investigated the characterization of air-dried native and denatured collagen films on the TCPS plates, and showed the alteration of pulmonary epithelial stem and stromal cells on these films with different nanostructures. Moreover, through the isolation of stem cells, we further studied the behaviors of colony cells in the self-renewal and differentiation which indirectly outlines the function of stromal cells.

Dupont-Gillain and co-workers have demonstrated that collagen organization varies with the properties of adsorbed surfaces, absorption duration, drying conditions and initial collagen concentration [21–25]. Different levels of fibrillogenesis were defined [26]. Filaments, formed from the linear assembly in a temperature-dependent initiation [27], are approximately 50 nm in diameter; fibrils, formed from the lateral assembly of filaments [27], are approximately 200 nm in diameter; and supramolecules, formed by fibril twists, are approximately up to 0.5  $\mu$ m in diameter. In this study, the degree of collagen assembly on native collagen films was controlled by the initial concentration. We operated all processes on standard TCPS plates by air-drying in a sterile hood, differing from the previous studies [12,13,24,25]. Our modified protocol enables the routine duplication of desirable collagen nanostructures from filaments, fibrils, to supramolecules, in a regular biological laboratory.

The heat-denatured collagen films, consisting of random coils unable to undergo filament assembly [14], exhibited no fibrillar collagen, except for some round-shaped aggregates discovered at high concentrations (0.62–3.88 mg/ml, Fig. 1C (i–iii)) [12,13]. Through utilizing knowledge of film preparation techniques and

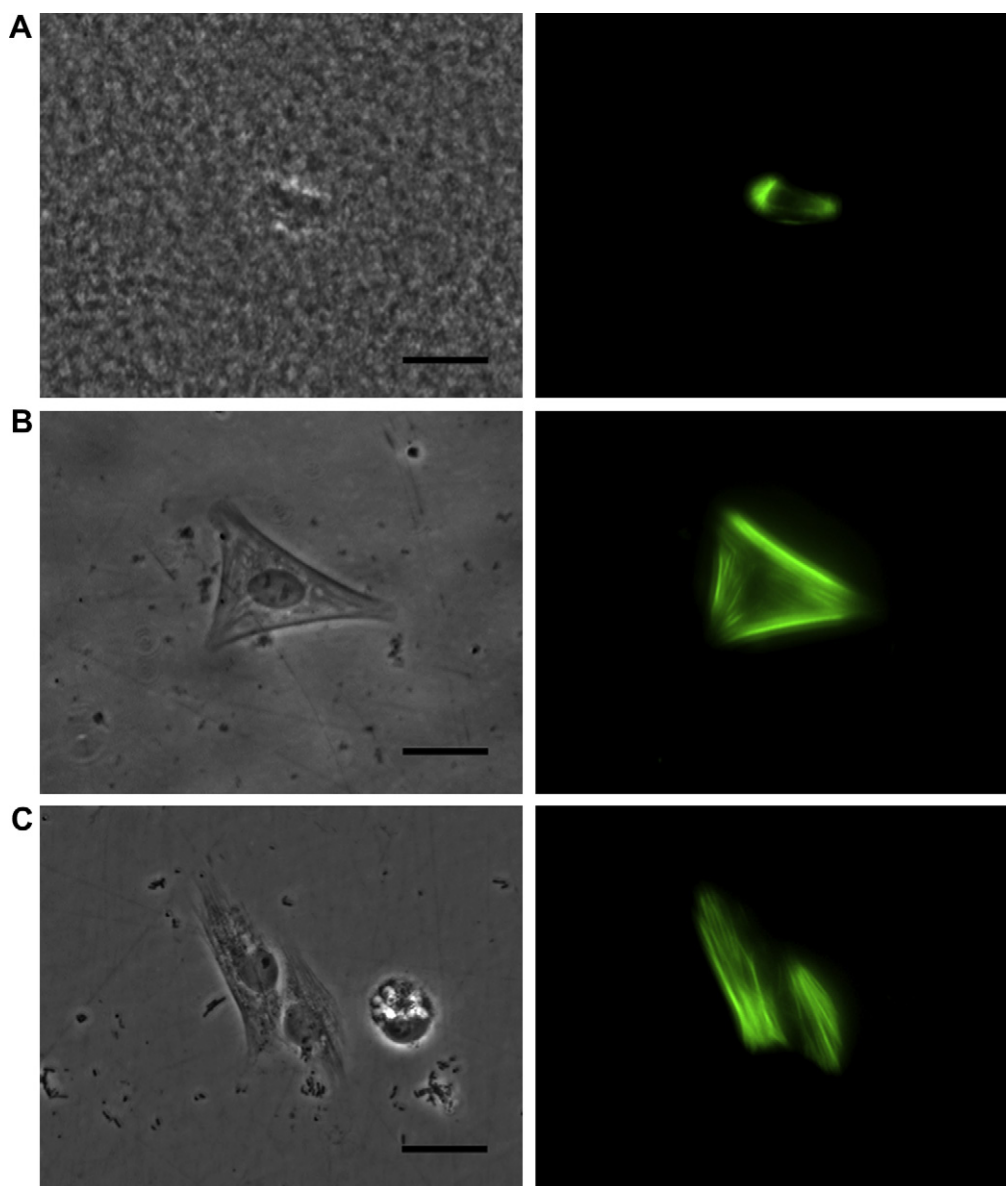


**Fig. 4.** Surface effects on the spreading of mesenchymal stromal cells in the pulmonary primary culture. The left column shows phase contrast images and the right column shows fluorescent immunostaining of stroma cells with antibodies against smooth muscle actin (FITC). Stroma cells were cultured on: A: native collagen with an initial concentration of 3.88 mg/ml; B: denatured collagen with an initial concentration of 3.88 mg/ml; C: bare TCPS cultured dish. All samples were secured on day four. All bars are 25  $\mu$ m.

characterization of surface properties, we are able to control the film thickness and nanostructure. This allows us to tackle the correlation of collagen structures with cell growth in a complicated primary culture system.

Cell shape and function are profoundly affected by the ECM, both during development and in the adult organism [28]. Ling et al.'s previous study has demonstrated that lung epithelial colony cells were fond of type I collagen and expressed stem cell markers, including Oct-4 SSEA-1, Sca-1 and cytokeratin-7 in a serum-free selective culture system [2]. Furthermore, the cells surrounding the epithelial colonies were stained positively for  $\alpha$ -smooth muscle actins, which are considered as a marker of mesenchymal cells. In this study, we utilized the Oct-4 marker, a typical marker of pluripotency for both mouse and human embryonic stem cells [29] (Fig. 2) and  $\alpha$ -smooth muscle actins (Fig. 4). Results indicate that cells cultured on both native and denatured collagen films do not alter the gene expression of Oct-4 and  $\alpha$ -smooth muscle actins,

suggesting the constancy in the pulmonary primary cell culture, and the nature of both colony cells and stromal cells can be maintained.

A disease named idiopathic pulmonary fibrosis is known to cause distortion of alveolar architecture, progressive decline in lung function and finally death [30]. It was understood to be concurrent with fibroblast accumulation, excessive collagen deposition and matrix remodeling. Recent studies have implicated insulin-like growth factor-I (IGF-I) in stimulation of collagen production and down-regulation of collagenase production [31]. In the present study, we systematically altered collagen quantity and fibrillar structures to observe the influences on pulmonary stem cells, which can undergo terminal differentiation into alveolar type 2 and type 1-like pneumocytes [2]. Although we could not provide direct evidence regarding the role of pulmonary stem cells in the disease, it is convincing that ECM remodeling should sufficiently modulate the subsequent tissue repair events by

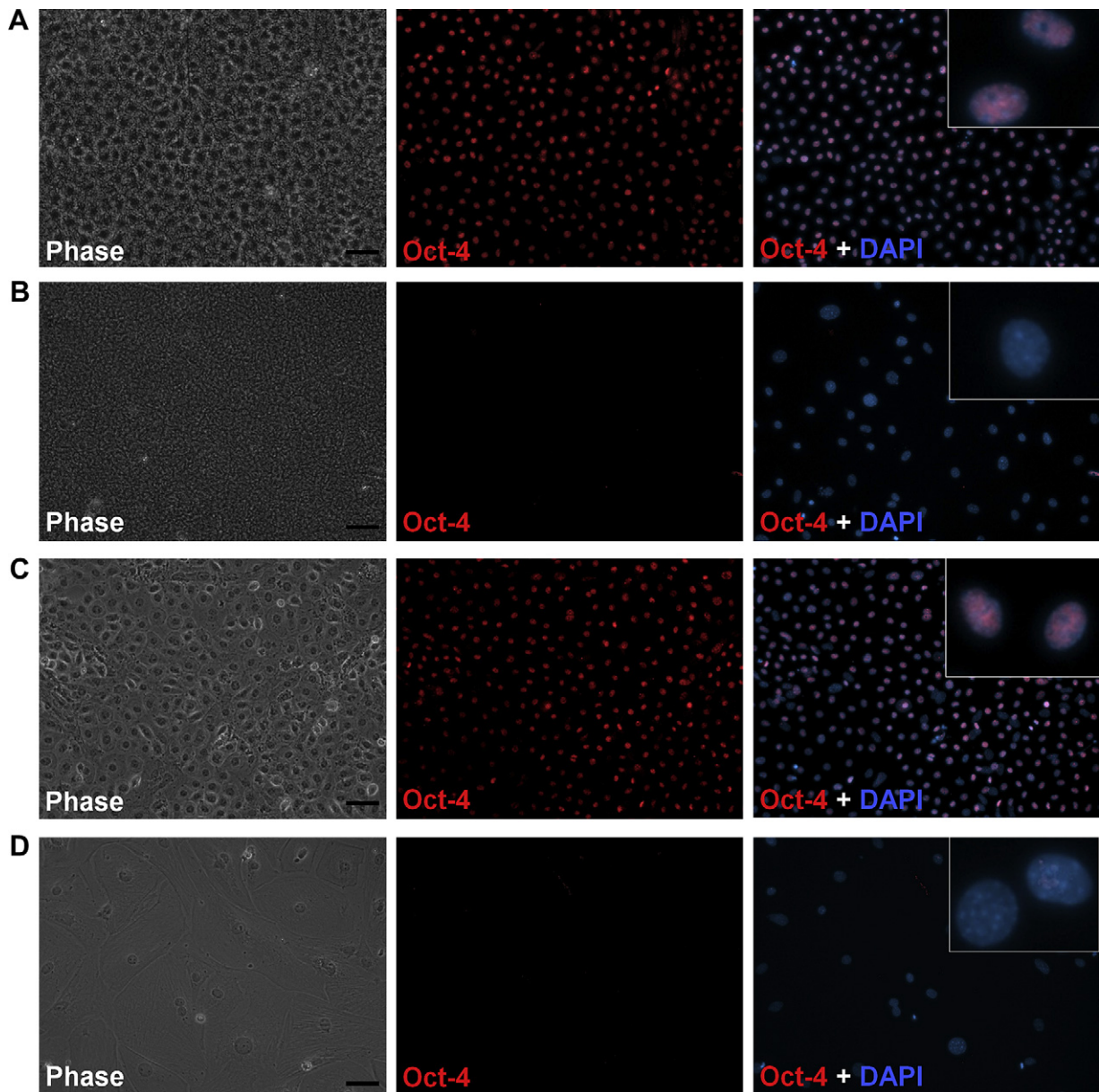


**Fig. 5.** Sorted stem/progenitor cells were then re-seeded on: (A) native collagen in DMEM containing 10% FBS. (B) native collagen in MCDB-201 without serum, for seven days. (C) denatured collagen in DMEM containing 10% FBS. (D) denatured collagen in MCDB-201 without serum, for seven days. All cell sets were stained with DAPI followed by immunostaining with Oct-4. All bars are 50  $\mu\text{m}$ . High magnification images are inserted in the late pictures of sets.

regeneration of stem cells. While cells were confluent on the native collagen-coated TCPS plate, colony density and size were both highly dependent on collagen fiber quantity. In contrast, stem cell colony density and size were consistently abundant on the denatured collagen that is analogous to the matrix metalloproteinase-treated collagen *in vivo* [32] (Fig. 3A). One would think that cell responses might be affected by collagen film bulk thickness. However, from the set of statistical colony cell numbers on denatured collagen films (Fig. 3A), the colony cell population did not depend on thickness (Fig. 1A). Hence, the effect of thickness on colony formation could be eliminated in this experiment, and the nanostructures of topmost collagen films are the important criterion for primary cell activities. It is clear that the adhesion and self-renewal of colony cells can be restricted on the fibril-abundant collagen films. In the meantime, on the native collagen films consisting of filaments and supramolecules, stromal cells

have low-spreading and disorganized cytoskeletal stress fibers (Fig. 4A). It is well known that integrins are responsible for the activation of growth-promoting signaling pathways as well as anchorage requirements, therefore cell survival and spreading are governed by integrin-mediated recognition sites [33,34]. Keresztes and co-workers reported that the space distribution of the fibrillar collagen's recognition sites may interfere with the organization of the cell-surface receptors [35]. Additionally, the other studies have also shown that SMCs failed to thrive when cultured on polymerized fibrillar collagen, which reflects the regulation of Cdk2 inhibitors [10,12,13]. For these reasons, we hypothesize that stromal cells play a crucial role in stem cell colony development. Moreover, in the cultivation of pre-sorted colony cells without stromal cells, we found that while cell fate is unaffected by collagen film nanostructures but impacted by medium components. Therefore, serum should be an alternative to functions of

stromal cell for colony cell self-renewal (Fig. 5A–D). It is known that niche cells underlying a basement membrane signal to stem cells to regulate differentiation and division in vivo. Proliferation, differentiation and survival of distinct progenitor populations in the hematopoiesis were discovered to depend on interactions with neighboring cells [36–40]. Similarly, secreted factors from niche cells play an instructive role in the differentiation of neural crest stem cells [41]. Thus, in this study, by utilizing manipulated nanostructures of collagen films, we further reveal that the growth of Oct-4<sup>+</sup> pulmonary epithelial colony cell population is arrested by the effects of the degree of collagen polymerization on adjacent mesenchymal stromal cells. These observations reflect that the ability of renewal of pulmonary epithelial stem cells may in turn be prohibited by the excessive production of collagen from fibroblasts as idiopathic pulmonary fibrosis arises in alveolae in vivo.

## 5. Conclusion

In this study, the correlation between pulmonary stem cells and their niches was examined by altering collagen thickness, nanostructures and medium conditions independently in both primary and pre-sorted colony cultures. Collectively, fibrillar collagen inhibits proliferation of pulmonary stem cells. This should be attributed to the regulating mechanisms through the interaction between the neighboring mesenchymal stromal cells and the surface nanostructured collagen films, rather than to the contact of stem cell with collagen surfaces and the bulk material properties in films. This is further evidenced by the fact that in a pre-sorted stem cell culture colony formation is independent on the textures of type I collagen, but only dependent on the presence of serum. This research is a step towards comprehending the relationship between the nanostructures of type I collagen and primary neonatal pulmonary cells, and provides insights into potential influences during collagen accumulation in vivo.

## Acknowledgements

We thank Academia Sinica, Taipei, Taiwan, for the funding support.

## Appendix

Figure with essential colour discrimination. Fig. 3 in this article difficult to interpret in black and white. The full colour image can be found in the on-line version, at doi:10.1016/j.biomaterials.2010.07.038.

## References

- [1] O'Neill A, Schaffer DV. The biology and engineering of stem-cell control. *Biotechnol Appl Biochem* 2004;40:5–16.
- [2] Ling TY, Kuo MD, Li CL, Yu AL, Huang YH, Wu TJ, et al. Identification of pulmonary Oct-4(+) stem/progenitor cells and demonstration of their susceptibility to SARS coronavirus (SARS-CoV) infection in vitro. *P Natl Acad Sci USA* 2006;103(25):9530–5.
- [3] Chen Y, Chan VS-F, Zheng B, Chan KY-K, Xu X, To LY-F, et al. A novel subset of putative stem/progenitor CD34(+) Oct-4(+) cells is the major target for SARS coronavirus in human lung. *J Exp Med* 2007;204(11):2529–36.
- [4] Wiles MV, Keller G. Multiple hematopoietic lineages develop from embryonic stem (ES) cells in culture. *Development* 1991;111(2):259–67.
- [5] Nakano T, Kodama H, Honjo T. Generation of lymphohematopoietic cells from embryonic stem cells in culture. *Science* 1994;265(5175):1098–101.
- [6] Choi D, Lee H-J, Jee S, Jin S, Koo SK, Paik SS, et al. In vitro differentiation of mouse embryonic stem cells: enrichment of endodermal cells in the embryoid body. *Stem Cells* 2005;23(6):817–27.
- [7] Li M, Pevny L, Lovell-Badge R, Smith A. Generation of purified neural precursors from embryonic stem cells by lineage selection. *Curr Biol* 1998;8(17):971–4.
- [8] Hui TY, Cheung KMC, Cheung WL, Chan D, Chan BP. In vitro chondrogenic differentiation of human mesenchymal stem cells in collagen microspheres: influence of cell seeding density and collagen concentration. *Biomaterials* 2008;29(22):3201–12.
- [9] Lanfer B, Seib FP, Freudenberg U, Stamov D, Bley T, Bornhauser M, et al. The growth and differentiation of mesenchymal stem and progenitor cells cultured on aligned collagen matrices. *Biomaterials* 2009;30(30):5950–8.
- [10] Koyama H, Raines EW, Bornfeldt KE, Roberts JM, Ross R. Fibrillar collagen inhibits arterial smooth muscle proliferation through regulation of Cdk2 inhibitors. *Cell* 1996;87(6):1069–78.
- [11] Elliott JT, Tona A, Jones PL, Plant AL. Highly reproducible fibrillar and non-fibrillar type I collagen surfaces induce a distribution of responses in smooth muscle cells. *Mol Biol Cell* 2002;13. 68A–68A.
- [12] Elliott JT, Tona A, Woodward JT, Jones PL, Plant AL. Thin films of collagen affect smooth muscle cell morphology. *Langmuir* 2003;19(5):1506–14.
- [13] Elliott JT, Woodward JT, Langenbach KJ, Tona A, Jones PL, Plant AL. Vascular smooth muscle cell response on thin films of collagen. *Matrix Biol* 2005;24(7):489–502.
- [14] Miles CA, Bailey AJ. Thermally labile domains in the collagen molecule. *Micron* 2001;32(3):325–32.
- [15] Jones PL, Crack J, Rabinovitch M. Regulation of tenascin-C, a vascular smooth muscle cell survival factor that interacts with the alpha(v)beta(3) integrin to promote epidermal growth factor receptor phosphorylation and growth. *J Cell Biol* 1997;139(1):279–93.
- [16] Curran S, Murray GI. Matrix metalloproteinases: molecular aspects of their roles in tumour invasion and metastasis. *Eur J Cancer* 2000;36(13):1621–30.
- [17] Ivaska J, Heino J. Adhesion receptors and cell invasion: mechanisms of integrin-guided degradation of extracellular matrix. *Cell Mol Life Sci* 2000;57(1):16–24.
- [18] Huang CJ, Tseng PY, Chang YC. Effects of extracellular matrix protein functionalized fluid membrane on cell adhesion and matrix remodeling. *Biomaterials*; 2010;. doi:10.1016/j.biomaterials.2010.05.076.
- [19] Oswald J, Steudel C, Salchert K, Joergensen B, Thiede C, Ehninger G, et al. Gene-expression profiling of CD34(+) hematopoietic cells expanded in a collagen I matrix. *Stem Cells* 2006;24(3):494–500.
- [20] Kommireddy DS, Sriram SM, Lvov YM, Mills DK. Stem cell attachment to layer-by-layer assembled TiO<sub>2</sub> nanoparticle thin films. *Biomaterials* 2006;27(24):4296–303.
- [21] Dupont-Gillain CC, Pamula E, Denis FA, De Cupere VM, Dufrene YF, Rouxhet PG. Controlling the supramolecular organization of adsorbed collagen layers. *J Mater Sci Mater Med* 2004;15(4):347–53.
- [22] Dupont-Gillain CC, Adriaensens Y, Derclaye S, Rouxhet PG. Plasma-oxidized polystyrene: wetting properties and surface reconstruction. *Langmuir* 2000;16(21):8194–200.
- [23] Dupont-Gillain CC, Rouxhet PG. AFM study of the interaction of collagen with polystyrene and plasma-oxidized polystyrene. *Langmuir* 2001;17(23):7261–6.
- [24] Dupont-Gillain CC, Jacquemart I, Rouxhet PG. Influence of the aggregation state in solution on the supramolecular organization of adsorbed type I collagen layers. *Colloid Surf B* 2005;43(3–4):179–86.
- [25] Jacquemart I, Pamula E, De Cupere VM, Rouxhet P, Dupont-Gillain CC. Nanostructured collagen layers obtained by adsorption and drying. *J Colloid Interface Sci* 2004;278(1):63–70.
- [26] Jones PL, Jones FS, Zhou B, Rabinovitch M. Induction of vascular smooth muscle cell tenascin-C gene expression by denatured type I collagen is dependent upon a beta 3 integrin-mediated mitogen-activated protein kinase pathway and a 122-base pair promoter element. *J Cell Sci* 1999;112(4):435–45.
- [27] Gelman RA, Poppke DC, Piez KA. Collagen fibril formation invitro – role of the non-helical terminal regions. *J Biol Chem* 1979;254(22):1741–5.
- [28] Adams JC, Watt FM. Regulation of development and differentiation by the extracellular-matrix. *Development* 1993;117(4):1183–98.
- [29] Saito S, Liu B, Yokoyama K. Animal embryonic stem (ES) cells: self-renewal, pluripotency, transgenesis and nuclear transfer. *Hum Cell* 2004;17:107–15.
- [30] Agusti C. American thoracic society/European respiratory society international multidisciplinary consensus classification of the idiopathic interstitial pneumonias. *Am J Respir Crit Care Med* 2002;166(3). 426–426.
- [31] Jones JL, Clemmons DR. Insulin-like growth-factors and their binding-proteins-biological actions. *Endocr Rev* 1995;16(1):3–34.
- [32] Davis GE. Affinity of integrins for damaged extracellular-matrix – alpha-v-beta-3 binds to denatured collagen type-I through rgd sites. *Biochem Biophys Res Commun* 1992;182(3):1025–31.
- [33] Chen CS, Mrksich M, Huang S, Whitesides GM, Ingber DE. Geometric control of cell life and death. *Science* 1997;276(5317):1425–8.
- [34] Neff JA, Tresco PA, Caldwell KD. Surface modification for controlled studies of cell–ligand interactions. *Biomaterials* 1999;20(23–24):2377–93.
- [35] Keresztes Z, Rouxhet PG, Remacle C, Dupont-Gillain C. Supramolecular assemblies of adsorbed collagen affect the adhesion of endothelial cells. *J Biomed Mater Res* 2006;76A(2):223–33.
- [36] Wagner W, Wein F, Roderburg C, Benes V, Diehlmann A, Krause U, et al. Adhesion of hematopoietic progenitor cells to human mesenchymal stromal cells as a model for interaction between stem cells and their niche. *Blood* 2006;108(11). 407A–407A.

- [37] Hall PA, Watt FM. Stem-cells – the generation and maintenance of cellular diversity. *Development* 1989;106(4):619–33.
- [38] Morrison SJ, Shah NM, Anderson DJ. Regulatory mechanisms in stem cell biology. *Cell* 1997;88(3):287–98.
- [39] Quesenberry PJ, Becker PS. Stem cell homing: rolling, crawling, and nesting. *P Natl Acad Sci USA* 1998;95(26):15155–7.
- [40] Wagner W, Saffrich R, Wirkner U, Eckstein V, Blake J, Ansorge A, et al. Hematopoietic progenitor cells and cellular microenvironment: behavioral and molecular changes upon interaction. *Stem Cells* 2005;23(8):1180–91.
- [41] Shah NM, Groves AK, Anderson DJ. Alternative neural crest cell fates are instructively promoted by TGF beta superfamily members. *Cell* 1996;85(3):331–43.